Research Article | Vol. 10, No. 6 | 1 Jun 2019 | BIOMEDICAL OPTICS EXPRESS 2784
Biomedical Optics EXPRESS

Absorption spectra of early stool from preterm infants need to be considered in abdominal NIRS oximetry

HELENE ISLER,[1,*] DANIEL SCHENK,[2] JÉRÔME BERNHARD,[2] STEFAN KLEISER,[1] FELIX SCHOLKMANN,[1] DANIEL OSTOJIC,[1] ALEXANDER KALYANOV,[1] LINDA AHNEN,[1] MARTIN WOLF,[1] AND TANJA KAREN[1]

[1]*Biomedical Optics Research Laboratory, Department of Neonatology, University Hospital Zürich, 8091 Zürich, Switzerland*
[2]*CARAG AG, 6340 Baar, Switzerland*
**helene.isler@usz.ch*

Abstract: Necrotizing enterocolitis (NEC) is the most common gastrointestinal emergency of the preterm infant. Low abdominal tissue oxygen saturation (StO_2) measured by near-infrared spectroscopy (NIRS) oximetry may be an early sign of NEC relevant for treating or even preventing NEC. However, current commercial NIRS oximeters provide inaccurate StO_2 readings because they neglect stool as an abdominal absorber. To tackle this problem, we determined the optical properties of faeces of preterm infants to enable a correct abdominal StO_2 measurement. In 25 preterm born infants (median age 31 0/7 ± 2 1/7 weeks, weight 1478 ± 511 g), we measured their first five stool probes with a VIS/NIR spectrometer and calculated the optical properties using the Inverse Adding Doubling (IAD) method. We obtained two absorption spectra representing *meconium* and *transitional stool*. Probabilistic cluster analysis correctly classified 96 out of 107 stool probes. The faeces spectra need to be considered to enable correct abdominal StO_2 measurements with NIRS oximetry.

1. Introduction

Near-infrared spectroscopy (NIRS) is able to measure regional tissue haemoglobin oxygen saturation (StO_2) non-invasively. Light in the near infrared (NIR) diagnostic window penetrates a few centimeters into tissue. In this range (probing volume), there is reportedly ~25% arterial and ~75% venous blood present [1], even though the arterial to venous ratio may be different than anticipated by most commercial oximeters [2,3]. Consequently, regional StO_2 represents a local oxygen balance (ratio between delivered and consumed oxygen). NIRS has been successfully applied for monitoring cerebral StO_2 in preterm infants (e.g [4,5]). Additionally, there is an increasing interest to monitor abdominal StO_2 to detect splanchnic ischemia, in particular in preterm infants who are at risk of developing necrotizing enterocolitis (NEC) [6–15]. However, abdominal NIRS readings have a clinically unacceptable low precision and a too high variability to reliably detect and monitor NEC [16,17].

Recent studies have applied commercially available NIRS oximeters (INVOS [8–10,15,18], InSpectra [14]) to the abdomen, although neither these sensors nor the algorithms were designed for abdominal measurements. Abdominal StO_2 shows much higher variability than cerebral and renal StO_2, and this variability decreases during the first weeks of life [18]. One probable reason for this high variability is that conventional NIRS oximetry does not account for the absorption of stool, which is present in the abdomen. For example, meconium staining reduces the measured intensity in red light, thus alters an optical signal [19]. Additionally, lavaging the lumen to perform reflectance spectrophotometry in the gastrointestinal tract was advised as stool presents interference [20]. Consequently, meconium

#356669 https://doi.org/10.1364/BOE.10.002784
Journal © 2019 Received 9 Jan 2019; revised 23 Mar 2019; accepted 23 Mar 2019; published 15 May 2019

Biomedical Optics EXPRESS

and early stool show an interference not to be neglected and are likely to cause the high variability in abdominal StO_2 readings [20–23].

The aim of this study is to determine the optical properties of stool and their change during the first days of life of preterm infants in order to incorporate them into future abdominal StO_2 measurements.

2. Methods

2.1 Study design

Twenty-five preterm infants were enrolled, excluding children with congenital malformations. With approval from the ethical committee (KEK-ZH-Nr. 2013-0558) and the written consent from the parents, the first five stool probes excreted by a preterm infant (gestational age < 35 weeks) were collected. Clinical information such as weight and gestational age were recorded together with an assessment of stool color, consistency and texture. Every stool probe was measured using a spectrophotometer within 24 hours whenever possible. Due to fast accumulation of diaper fillings, measurements were in some cases delayed with the latest measurement starting 42 hours after excretion.

2.2 Measurement procedure

Each stool probe was removed from the diaper with a spatula and placed into four demountable, cylindrical quartz glass cuvettes (Hellma Analytics, Müllheim, Germany) with different thicknesses (0.1, 0.2, 0.5 and 1.0 mm). If not enough stool was available, the medium thicknesses 0.2 mm and/or 0.5 mm were filled first. Stool characteristics such as texture, color and homogeneity were recorded. Homogeneous green stool probes with no or very few curd beads were classified as *meconium*, whereas stool probes with numerous curd beads and colors in the range from green to brown and yellow were classified as *transitional stool*. The number of curd beads was registered as mottle level in the categories *no beads*, *few beads*, *many beads* and *no more beads*.

The stool probes were analyzed with a spectrophotometer (UV 1601, Shimadzu Corporation, Kyoto, Japan). Three different measurement series were conducted: unscattered transmittance (U) with the standard sample holder and total transmittance (T) as well as total reflectance (R) with an integrating sphere. The probed wavelength range was 600 nm to 1000nm. Every measurement was repeated three times per sample (delivering $M_{\mathrm{U},j}, M_{\mathrm{T},j}, M_{\mathrm{R},j}$ with $j = 1,2,3$). For further analysis, the median data set $M_{X,j}, X \in \{U,R,T\}, j \in \{1,2,3\}$ with the largest number of measurement points in between the two other curves was employed, greatly reducing computation time [24].

2.3 Data analysis

Established methods to assess optical properties from spectrometric measurements are the Kubelka Munk theory and Monte Carlo simulations as well as the (inverse) adding doubling method [25,26]. Kubelka Munk assumes isotropic scattering and perfectly diffuse illumination as well as matched boundary conditions, whereas Monte Carlo methods are computationally expensive. Inverse adding doubling (IAD) was the method (version 3-9-11, https://omlc.org/software/iad/) of our choice to analyze the stool spectra since this method is valid for all ratios of μ_s' to μ_a coefficients, accommodates to arbitrary scattering phase functions, and accounts for internal reflections at the samples boundaries [27]. IAD iteratively estimates a set of optical properties and runs a Monte Carlo employing the adding doubling method [28,29] until the calculated total reflectance (R), total and unscattered transmittance (T, U) match the measured values [30,31]. These Monte Carlo simulations solve the radiative transfer equation and hold true for homogeneous, smooth samples with an infinite plane-parallel slab tissue geometry, assuming time independent light distribution and ignoring

Biomedical Optics EXPRESS

polarization effects. With a fixed refractive index n, IAD extracts from the measurements $M_{X,j}$ the absorption μ_a, reduced scattering μ_s' and anisotropy g spectra. To correct abdominal NIRS readings for stool interference, only the μ_a spectra are of interest. However, as the full data set, including μ_s' and g spectra, may be of interest to other fields, the complete data set is represented in this work. We assume a refractive index of $n = 1.33$ as the main constituents of meconium, water [32,33] and intestinal mucosa [34], exhibit this value. If the stool was optically very dense without light transmittance $\left(M_T(\lambda_k) = 0, \lambda_k \in \{600\text{nm}, 1000\text{nm}\}\right)$, the respective sample was rejected. Furthermore, the noisiest 5% of all complete spectra were excluded from further analysis. If multiple stool probes per diaper were available, the spectra from the thickest sample was analyzed further, because it has the highest signal to noise ratio.

2.3.1 Water content correction

When chyme passes the large intestine, water is being withdrawn and reabsorbed. The longer chyme stays within the large intestine before excretion, the more compacted it becomes. This delivers a broad range of stool densities, resulting in μ_a and μ_s' spectra with a large intermeasurement variability. In this work, we are not interested in the water content of the stool probe, but the μ_a spectra of stool from preterm infants. We minimized the influence of varying water content by applying the multiplicative signal correction (MSC) [35–37]. All absorption spectra were modelled as $\mu_{a,m,k} = a_m + b_m \times \overline{\mu}_{a,k} + e_{m,k}$ with m being the sample and k being the wavelength number. The average μ_a at the k^{th} wavelength is $\overline{\mu}_{a,k} = N^{-1}\sum_{j=1}^{N}\mu_{a,j,k}$. The a_m, b_m coefficients were estimated individually for each sample, whereas the variable $e_{m,k}$ describes the model error. MSC transforms $\mu_{a,m,k}$ to $\mu^*_{a,m,k} = \left(\mu_{a,m,k} - a_m\right)/b_m$.

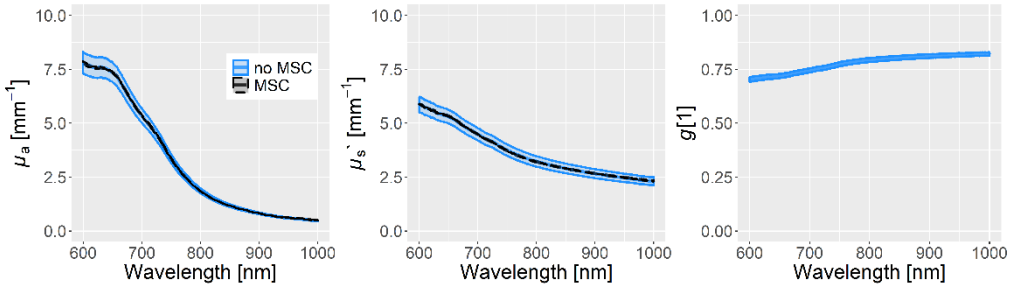

Fig. 1. The optical spectra estimated by IAD are shown in blue for all 107 complete stool spectra through their mean and standard error of the mean (SEM). As the stool probes differed in water content, which masked the μ_a and μ_s' features we are interested in, a multiplicative signal correction (MSC) was applied.

2.3.2 Principal component analysis and probabilistic clustering

To identify structures within the μ_a spectra of the stool probes, a principal component analysis (PCA) was performed on the MSC μ_a curves. The scores and loadings from the mean centered μ_a matrix $\mathbf{M}$ were computed by applying the singular value decomposition $\mathbf{M} = (\mathbf{UD})\mathbf{V}^T$ in the R statistics software (R version 3.5.1 [38]). The new set of base vectors is equal to $\mathbf{V}$, they are called loadings and are referred to as principal components (*PC*) in this work. The new coordinates are called scores and given by $\mathbf{UD}$. To investigate the μ_a spectra in the *PC* space on structures, a probabilistic clustering method was employed. The Bayesian Information Criterion [39] (BIC) was applied to estimate the optimal number of clusters describing the data structure assuming Gaussian mixture models. Subsequently, the probabilistic clustering method from the *mclust* package [40,41] identified the number of clusters proposed by BIC.

Biomedical Optics EXPRESS

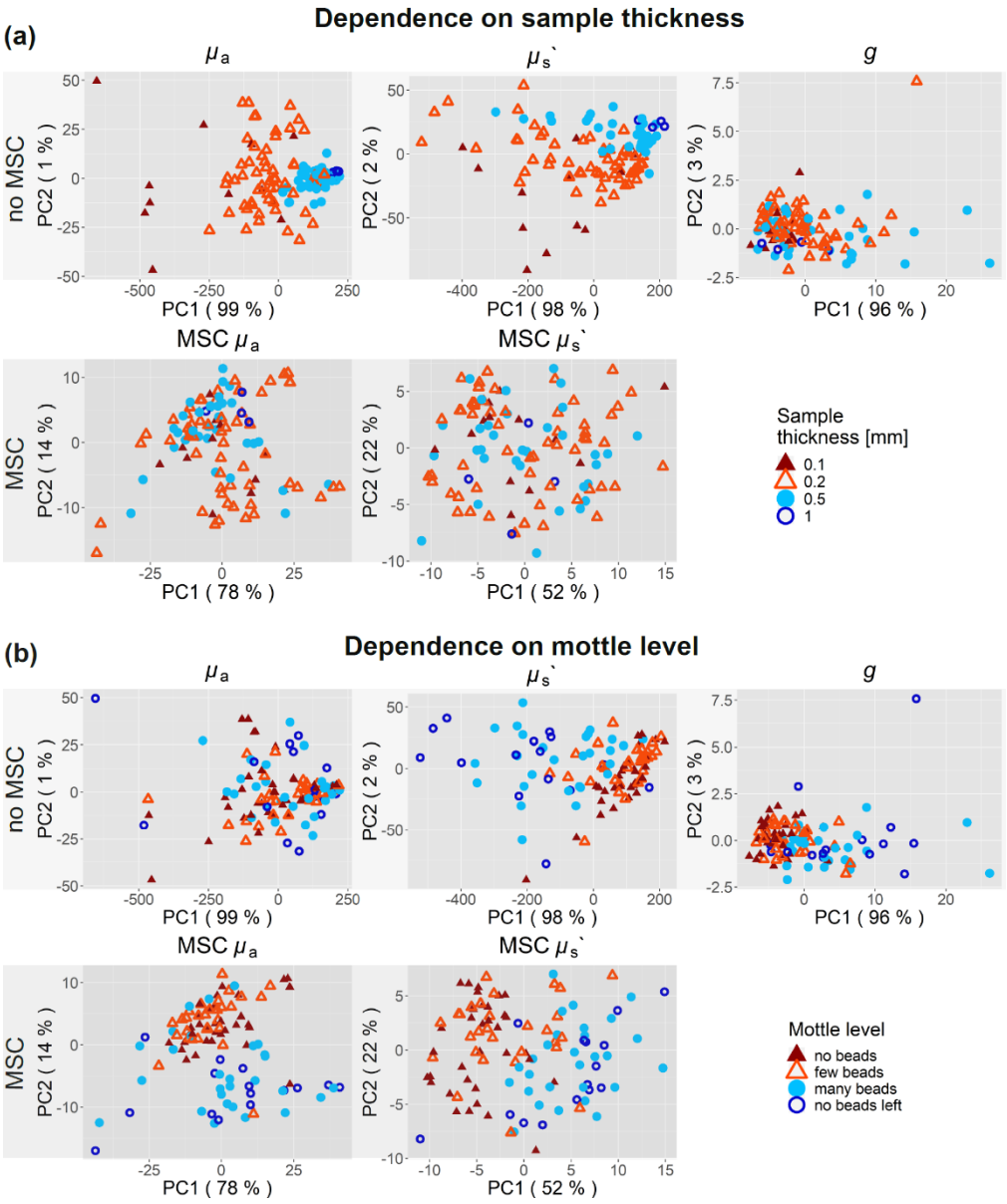

Fig. 2. PCA of all 107 stool spectra, with and without MSC. The scores are shown for the first two *PC*s for μ_a, μ_s' and *g*. (a) The sample thickness and (b) mottle level of the stool are presented with colors. (a) The color coding varies from red to blue with increasing thickness. Humid stool probes were more transparent and hence data from thicker cuvettes more likely to be included. MSC removes the influence on sample thickness in PCA as shown in the lower subplots, effectively removing the influence of varying water content. (b) *Meconium* entails the probes with zero up to few beads, colored in dark and light red. *Transitional stool* probes contain many beads or have no more beads left, they are shown in light and dark blue. MSC uncovers the influence of the mottle level on PCA in μ_a as seen in the bottom left subplot.

3. Results

The first 5 stool probes from 25 infants were aimed for. Thirteen stool probes showed incomplete spectra and were excluded. Five diapers were accidentally discarded. Two diapers contained more slime than stool and were excluded as well. Lastly, for two children there

Biomedical Optics EXPRESS

were 6 diapers analyzed as the final two diapers were filled within the short time frame of 30 minutes. Finally, from a total of 125 diapers, 107 diapers were analyzed and are presented in this paper.

The MSC scaled the stool μ_a and μ_s' spectra towards the mean stool μ_a and μ_s' spectra but preserved the shape. The result can be seen in Fig. 1. To test whether the MSC removes meaningful information from the data, principal component analysis (PCA) was performed on the μ_a and μ_s' spectra with and without MSC. The resulting scores for both PCAs are shown with respect to sample thickness and mottle level (Fig. 2). MSC removes the influence of sample thickness on the scores distribution and uncovers the influence of mottle level (i.e. stool development) for the μ_a and μ_s' spectra.

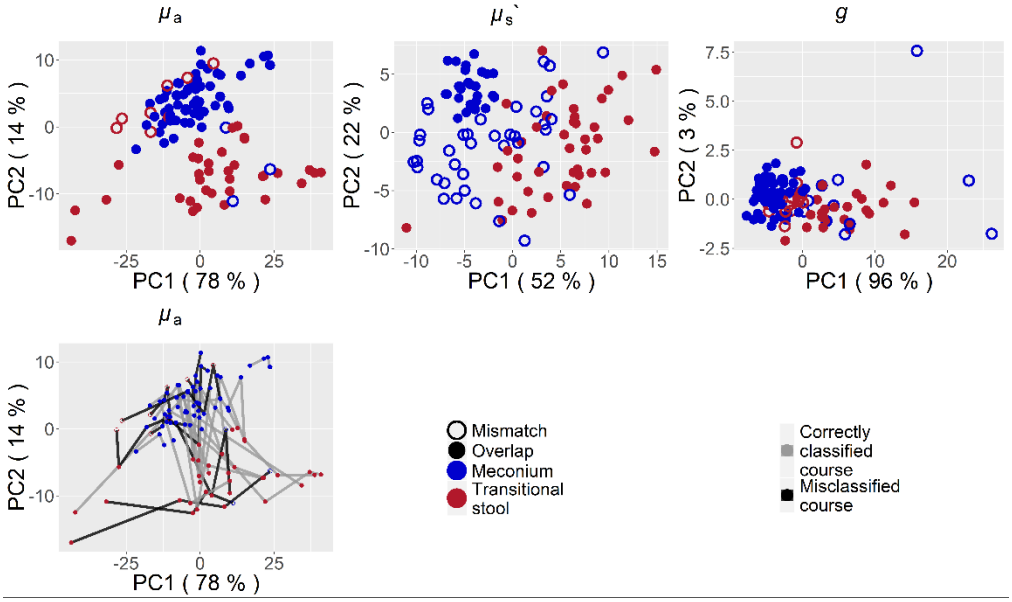

Fig. 3. PCA of all 107 MSC stool μ_a, μ_s' and g spectra (a,b and c). A probabilistic cluster analysis was carried out on the scores of the first two principal components (PC), delivering two clusters for each property. In case of the μ_a spectra, these clusters coincide for 90% of all stool probes with the classification of stool into *meconium* (blue) and *transitional stool* (red). Following the development of μ_a from *meconium* to *transitional stool*, the clustering predicts a correct course for 17 out of 25 children (d).

Continuing further analysis with MSC spectra only, *PC1* and *PC2* describe 92% of all variance in the μ_a data. Accordingly, the first two *PCs* are most likely to contain clustering information. The BIC proposes a model with two clusters on *PC1* and *PC2* scores. These clusters were identified with the mclust [40,41] package and shown in Fig. 3. The two clusters coincide for 96 from a total of 107 stool probes with the eye-sight classification into *meconium* and *transitional stool*. Table 1 shows the classification and probabilistic cluster analysis along with the gestational age and the preterm infants' weight. This demonstrates that the differences in stool color and texture as seen in the visible wavelength range are apparent in the near-infrared spectrum as well. The median μ_a, μ_s' and g spectra of both stool types, *meconium* and *transitional stool*, are plotted with their standard error in Fig. 4. The μ_a curves of haemoglobin are added for comparison [42]. Probabilistic clustering on *PC1* and *PC2* of the uncorrected μ_a spectra showed no agreement with neither sample humidity, the child's age, GA nor with the stool's age at time of measurement. Clustering information on *PC1* and *PC2* of the uncorrected data coincides with the stool types (*meconium*, *transitional stool*) for 53% of all samples in contrast to 90% for MSC corrected data.

Biomedical Optics EXPRESS

Table 1. Data of all study subjects concerning gestational age, weight and stool probes measured. The number of stool probes measured in each category and their identification (ID) by the probabilistic clustering method is given in comparison to classification (class) by eye-sight.

child	GA [weeks]	weight [g]	meconium [ID / class samples]	transitional stool [ID / class samples]
1	32 1/7	1960	3/3	0/0
2	33 1/7	1450	4/4	0/1
3	33 0/7	1680	2/2	1/1
4	33 0/7	2000	2/2	1/1
5	28 4/7	1200	2/2	3/3
6	30 6/7	1370	4/4	2/2
7	32 5/7	1710	2/2	3/3
8	32 5/7	1480	2/2	3/3
9	34 3/7	2760	4/4	1/1
10	32 5/7	1750	4/4	0/1
11	32 5/7	1340	2/2	3/3
12	29 6/7	1300	0/1	3/3
13	29 6/7	1200	0/1	3/3
14	31 1/7	1560	1/1	0/0
15	29 5/7	1165	3/3	1/2
16	26 3/7	580	1/1	1/1
17	29 6/7	1280	1/2	2/2
18	34 4/7	2280	3/3	0/2
19	26 6/7	1000	2/2	1/2
20	26 6/7	840	3/3	2/2
21	32 4/7	2310	1/1	2/2
22	29 6/7	1350	3/3	2/2
23	29 6/7	1390	4/4	1/1
24	30 1/7	600	5/5	0/0
25	30 1/7	1400	3/3	0/2
Mean ± Std	31 0/7 ± 2 1/7	1478 ± 511	61/64	35/43

4. Discussion

We determined the μ_a spectra of early stool probes from preterm infants in the NIR light. We discovered two different spectra coinciding with the stool types *meconium* and *transitional stool*. IAD was the method of our choice due to its broad applicability. Nevertheless, IAD poses certain requests on the spectroscopic measurements regarding sample size, homogeneity, thickness, sample holders and beam profile of the spectroscopic device. Most requirements were met, but our beam profile differed from the requested one and sample homogeneity was partly not fulfilled. Early meconium and late transitional stool probes are homogeneous, but the intermediate stool probes contain inhomogeneities in the form of curd beads. We obtained inhomogeneities in 57 samples (i.e. 53% of our samples). However, according to our assessment we are of the opinion that the inhomogeneities average out considering the rectangular beam profile (1×9 mm^2) and sample size (thickness of 0.1, 0.2, 0.5 and 1.0 mm, diameter of 15 mm) being larger than the average inhomogeneity as well as the large number of stool probes being analyzed. Samples with inhomogeneities deliver properties with a higher

Biomedical Optics EXPRESS

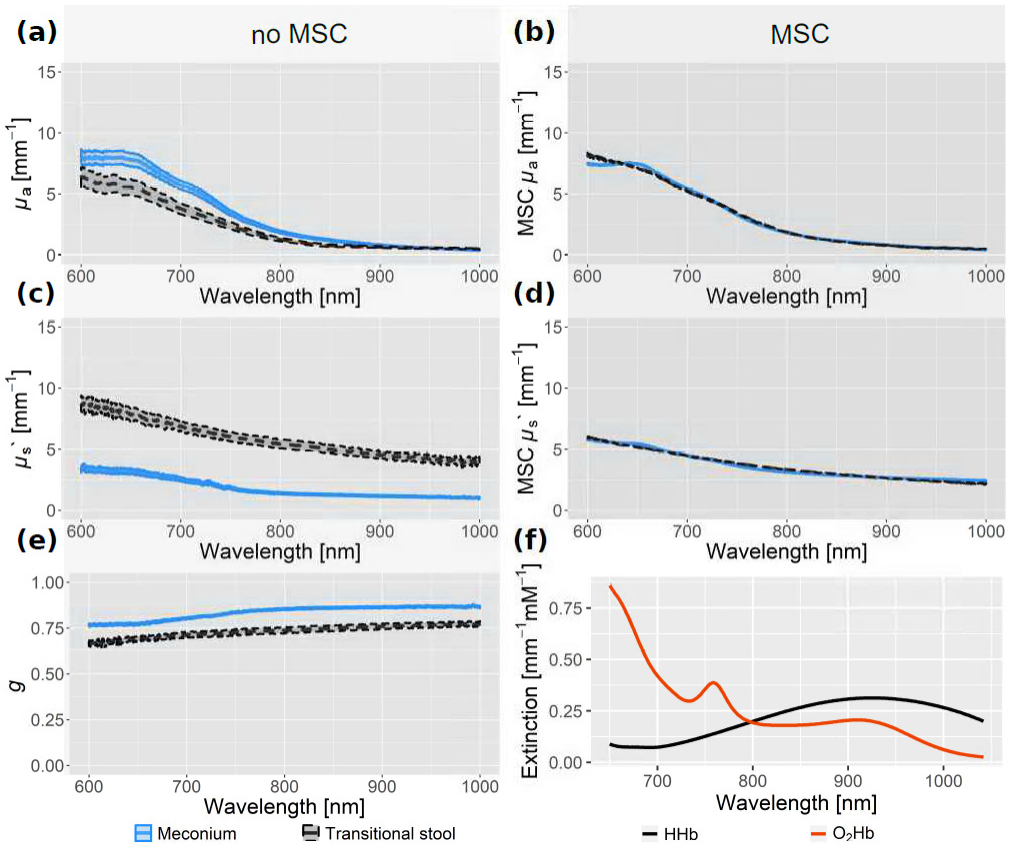

Fig. 4. The median μ_a, μ_s' and g spectra for 107 *meconium* and *transitional stool* probes are shown with their standard error. The absorption μ_a, reduced scattering μ_s' and anisotropy g coefficients are shown without (a, c, e) and with (b, d) multiplicative signal correction (MSC). Extinction coefficients of oxy- and deoxy-haemoglobin are shown in (f) for comparison.

variation but still blend into the development from early meconium to late transitional stool. In addition, IAD assumes a circular beam profile hitting the stool probe, whereas our beam profile has a rectangular cross section. Although IAD was informed with the correct sample area covered by light, the altered shape places some portions of light closer to the sample edge and the integrating sphere opening than anticipated by IAD. This results in a larger loss of light at the sphere opening and sample border than IAD will predict, which in turn will be interpreted as a higher sample extinction coefficient. However, stool μ_a in general showed high values, leaving only little room for signal loss at the border and its misinterpretation. Finally, IAD bases its Monte Carlo routine on a refractive index given by the user. The index of refraction was chosen to be n = 1.33 as water [32,33] and intestinal mucosa [34] show the same value and depict the main constituents of meconium. Nevertheless, the true refractive index of stool is to the best of our knowledge not known and can be larger than assumed due to other compounds such as biliverdin and bilirubin [43]. To investigate the possible influence of different refractive index values, we reran the complete analysis also on n = 1.43. We obtained the same stool μ_a features as for n = 1.33. The mean μ_a curves for meconium as well as transitional stool from the analysis with the smaller refractive index can be scaled and translated into the analysis with the larger refractive index.

The stool probes were classified by eye into either *meconium* or *transitional stool*. There is an uncertainty regarding the crossing from meconium to transitional stool as it is not clear

Biomedical Optics EXPRESS

where exactly meconium stops, and transitional stool starts. Consequently, probabilistic clustering is not expected to fully overlap with the eye-classification into the two stool types.

Preterm infants at our neonatal ward are initially fed with formula, which is gradually replaced with human milk. During the first days of life, the gastrointestinal tract evolves to stomach nutrition, which changes the stool pattern, texture and color. The changes in the near infrared spectrum for the first five stool probes were observed as they evolve from meconium to transitional stool. We have investigated the first steps in stool development and found that preterm infants' stool evolves in varying speed. Furthermore, we observed no clustering information on neither child gestational age nor child weight at time of birth. We found no change in spectral μ_a arising from the waiting time between stool excretion and spectral analysis.

Are there other absorbers that may interfere with a correct StO_2 measurement? One strong absorber is melanin. Since most NIRS devices are based on a multidistance approach, since the multidistance measurements were shown to cancel the influence of superficial tissue [44,45], and since melanin is located very superficially, we do not expect that melanin will lead to inaccurate StO_2 readings. At most melanin will lead to a decreased light intensity at the detectors and this may increase the noise level slightly. Another such molecule may be bilirubin. But the absorption of bilirubin is high in the blue region and negligible in the NIR region [46]. Therefore, we do not expect any interference of bilirubin. Indeed, hemoglobin is by far the strongest absorber in tissue in the NIR with the exception of the abdomen, where meconium/stool absorbs NIR light strongly.

Larger blood vessels are known to act similar to black holes: they absorb all the light entering the blood vessel. Thus, they do not contribute to changes in the NIRS signal [47]. We expect that larger (>1mm) lumps of dense stool will be acting similarly. Such lumps will probably interfere little with a correct measurement of StO_2. However, we expect that there will also be unknown quantities of small meconium/stool particles or meconium/stool of low optical density, which will definitely interfere with a correct StO_2 measurement. Only an appropriate correction for stool may prevent such errors.

The spectra of *meconium* and *transitional stool* show a trend in μ_a opposite to oxy-haemoglobin. Consequently, if an oximeter measures on the abdomen and stool is present, this leads to erroneous readings of the oxy-haemoglobin concentration and a falsely low StO_2. This effect depends on the set of wavelengths of the light sources, but arguably will affect any NIRS device. If the μ_a spectra for *meconium* and *transitional stool* are considered, this will enable to correct NIRS oximeter readings.

In principle, it would be possible to reanalyze existing NIRS data, if the raw intensities were available and if the employed instrument provided raw intensities for at least three wavelengths. Three wavelengths are sufficient if they are placed at wavelengths, where meconium and transitional stool have similar absorption coefficients. Otherwise at least four appropriate wavelengths are necessary. Unfortunately, most commercial instruments do not provide raw intensities. Furthermore, it would be possible to determine the concentration of stool in the abdomen. However, no commercially available clinical NIRS instrument is able to quantify μ_a so far and in addition, the absorption spectrum of meconium/stool varies tremendously depending on the water concentration. But it should be possible to estimate the presence of stool in categories such as low, medium or high.

5. Conclusion and outlook

We have determined the μ_a spectra of meconium and transitional stool and found a strong absorption in the NIR light. This is very likely to disturb traditional oximeter readings and explain the observed high variability of such readings [14]. Probabilistic cluster analysis discovered differences between the two stool types. These μ_a spectra will be employed to correct abdominal oximeter readings for the interference of stool Abdominal NIRS measurements on at least three appropriate wavelengths are required to consider meconium

Biomedical Optics EXPRESS

and/or transitional stool spectra. Not taking the absorption spectral information of preterm stool into account when determining StO_2 with NIRS oximetry on the preterm abdomen will lead to false StO_2 values. Studies that missed this critical aspect in the abdominal NIRS measurements need to be reevaluated and reinterpreted.

Furthermore, expanding existing NIRS oximeter models to recognize the presence of *meconium* and *transitional stool* not only allows for stool-corrected abdominal StO_2, but also for the detection of stool. Similarly to classifying the interference of stool on abdominal NIRS measurements [22], the presence of stool can be estimated to be *high*, *medium* or *low*. Combining this rating with variations in time may enable conclusions on gut motility and constipation. This will promote NIRS oximetry as a non-invasive and cost-efficient tool to monitor the abdomen of critically ill preterm infants.

Funding

InnoSuisse (CTI number 14786.1 PFLS-LS); Swiss Cancer Research (KFS-3732-08-2015); the SwissTrans-Med project ONIRIUS; the Clinical Research Priority Programs (CRPP) Tumor Oxygenation TO2; Molecular Imaging Network Zürich MINZ of University of Zürich and the Swiss National Science Foundation (project 159490).

Acknowledgments

We thank the medical staff of the neonatal unit of USZ for their cooperation, dedication and engagement. Furthermore, we thank Brigitte Koller and Sue Behre for fruitful discussions and expertise. Finally, we like to thank the parents whose children participated in the study.

Disclosures

MW, SK, DO: OXYPREM AG (I,S), JB, DS: CARAG AG (F,E,P,S)

References

1. V. Pollard, D. S. Prough, A. E. DeMelo, D. J. Deyo, T. Uchida, and H. F. Stoddart, "Validation in volunteers of a near-infrared spectroscope for monitoring brain oxygenation in vivo," Anesth. Analg. **82**(2), 269–277 (1996).
2. H. Sørensen, N. H. Secher, and P. Rasmussen, "A note on arterial to venous oxygen saturation as reference for NIRS-determined frontal lobe oxygen saturation in healthy humans," Front. Physiol. **4**, 403 (2014).
3. H. M. Watzman, C. D. Kurth, L. M. Montenegro, J. Rome, J. M. Steven, and S. C. Nicolson, "Arterial and venous contributions to near-infrared cerebral oximetry," Anesthesiology **93**(4), 947–953 (2000).
4. M. Wolf, G. Naulaers, F. van Bel, S. Kleiser, and G. Greisen, "Review: A review of near infrared spectroscopy for term and preterm newborns," J. Near Infrared Spectrosc. **20**(1), 43–55 (2012).
5. L. M. L. Dix, F. van Bel, W. Baerts, and P. M. A. Lemmers, "Comparing near-infrared spectroscopy devices and their sensors for monitoring regional cerebral oxygen saturation in the neonate," Pediatr. Res. **74**(5), 557–563 (2013).
6. M. D. Wider, "Hemodynamic Management and Regional Hemoglobin Oxygen Saturation (rSO2) of the Brain, Kidney and Gut," J. Perinatol. Neonatol. **22**, 57–60 (2009).
7. P.-M. Fortune, M. Wagstaff, and A. J. Petros, "Cerebro-splanchnic oxygenation ratio (CSOR) using near infrared spectroscopy may be able to predict splanchnic ischaemia in neonates," Intensive Care Med. **27**(8), 1401–1407 (2001).
8. S. M. Bailey, K. D. Hendricks-Munoz, and P. Mally, "Cerebral, renal, and splanchnic tissue oxygen saturation values in healthy term newborns," Am. J. Perinatol. **31**(4), 339–344 (2014).
9. N. P. Bernal, G. M. Hoffman, N. S. Ghanayem, and M. J. Arca, "Cerebral and somatic near-infrared spectroscopy in normal newborns," J. Pediatr. Surg. **45**(6), 1306–1310 (2010).
10. V. Bozzetti, G. Paterlini, Fv. Bel, G. H. A. Visser, L. Tosetti, D. Gazzolo, and P. E. Tagliabue, "Cerebral and somatic NIRS-determined oxygenation in IUGR preterm infants during transition," J. Matern. Fetal Neonatal Med. **29**(3), 443–446 (2016).
11. I. J. Zamora, B. Stoll, C. G. Ethun, F. Sheikh, L. Yu, D. G. Burrin, M. L. Brandt, and O. O. Olutoye, "Low Abdominal NIRS Values and Elevated Plasma Intestinal Fatty Acid-Binding Protein in a Premature Piglet Model of Necrotizing Enterocolitis," PLoS One **10**(6), e0125437 (2015).
12. A. N. Gay, D. A. Lazar, B. Stoll, B. Naik-Mathuria, O. P. Mushin, M. A. Rodriguez, D. G. Burrin, and O. O. Olutoye, "Near-infrared spectroscopy measurement of abdominal tissue oxygenation is a useful indicator of intestinal blood flow and necrotizing enterocolitis in premature piglets," J. Pediatr. Surg. **46**(6), 1034–1040 (2011).

Biomedical Optics EXPRESS

13. G. E. Stapleton, B. K. Eble, H. A. Dickerson, D. B. Andropoulos, and A. C. Chang, "Mesenteric oxygen desaturation in an infant with congenital heart disease and necrotizing enterocolitis," Tex. Heart Inst. J. **34**(4), 442–444 (2007).
14. A. K. Patel, D. A. Lazar, D. G. Burrin, E. O. B. Smith, T. J. Magliaro, A. R. Stark, M. L. Brandt, I. J. Zamora, F. Sheikh, A. C. Akinkuotu, and O. O. Olutoye, "Abdominal near-infrared spectroscopy measurements are lower in preterm infants at risk for necrotizing enterocolitis," Pediatr. Crit. Care Med. **15**(8), 735–741 (2014).
15. J. Cortez, M. Gupta, A. Amaram, J. Pizzino, M. Sawhney, and B. G. Sood, "Noninvasive evaluation of splanchnic tissue oxygenation using near-infrared spectroscopy in preterm neonates," J. Matern. Fetal Neonatal Med. **24**(4), 574–582 (2011).
16. S. M. Bailey and P. V. Mally, "Review of splanchnic oximetry in clinical medicine," J. Biomed. Opt. **21**(9), 091306 (2016).
17. S. Oh, C. Young, N. Gravenstein, S. Islam, and J. Neu, "Monitoring technologies in the neonatal intensive care unit: implications for the detection of necrotizing enterocolitis," J. Perinatol. **30**(11), 701–708 (2010).
18. S. McNeill, J. C. Gatenby, S. McElroy, and B. Engelhardt, "Normal cerebral, renal and abdominal regional oxygen saturations using near-infrared spectroscopy in preterm infants," J. Perinatol. **31**(1), 51–57 (2011).
19. N. Johnson, V. A. Johnson, J. Bannister, and H. McNamara, "The effect of meconium on neonatal and fetal reflectance pulse oximetry," J. Perinat. Med. **18**(5), 351–355 (1990).
20. S. Friedland, D. Benaron, I. Parachikov, and R. Soetikno, "Measurement of mucosal capillary hemoglobin oxygen saturation in the colon by reflectance spectrophotometry," Gastrointest. Endosc. **57**(4), 492–497 (2003).
21. M. M. Said, N. Niforatos, and K. Rais-Bahrami, "Validation of near infrared spectroscopy to measure abdominal somatic tissue oxygen saturation in neonates," J. Neonatal Perinatal Med. **6**(1), 23–30 (2013).
22. M. M. Said, N. Niforatos, and K. Rais-Bahrami, "Testing a new NIRS method to measure regional mesenteric tissue oxygen saturation in preterm infants that compensates for meconium and transitional stool interference," J. Neonatal Perinatal Med. **5**, 9–16 (2012).
23. A. Thompson, P. Benni, S. Seyhan, and R. Ehrenkranz, "Meconium and Transitional Stools May Cause Interference with Near-Infrared Spectroscopy Measurements of Intestinal Oxygen Saturation in Preterm Infants," in *Oxygen Transport to Tissue XXXIV*, W. J. Welch, F. Palm, D. F. Bruley, and D. K. Harrison, eds. (Springer New York, New York, NY, 2013), pp. 287–292.
24. H. Isler, C. Germanier, L. Ahnen, J. Jiang, S. Lindner, A. Di Costanzo Mata, T. Karen, S. Sánchez Majos, M. Wolf, and A. Kalyanov, "Optical properties of mice's stool in 550 to 1000 nm wavelength range," J. Biophotonics **11**(2), e201700076 (2018).
25. P. Kubelka, "New contributions to the optics of intensely light-scattering materials," J. Opt. Soc. Am. **38**(5), 448–457 (1948).
26. B. G. Yust, L. C. Mimun, and D. K. Sardar, "Optical absorption and scattering of bovine cornea, lens, and retina in the near-infrared region," Lasers Med. Sci. **27**(2), 413–422 (2012).
27. I. J. Bigio and S. Fantini, *Quantitative Biomedical Optics* (Cambridge University Press, 2016).
28. S. A. Prahl, M. J. C. van Gemert, and A. J. Welch, "Determining the optical properties of turbid mediaby using the adding-doubling method," Appl. Opt. **32**(4), 559–568 (1993).
29. S. A. Prahl, "The Adding-Doubling Method," in *Optical-Thermal Response of Laser-Irradiated Tissue*, A. J. Welch and M. J. C. Van Gemert, eds. (Springer US, Boston, MA, 1995), pp. 101–129.
30. J. W. Pickering, C. J. M. Moes, H. J. C. M. Sterenborg, S. A. Prahl, and M. J. C. van Gemert, "Two integrating spheres with an intervening scattering sample," J. Opt. Soc. Am. A **9**(4), 621–631 (1992).
31. S. A. Prahl, "Everything I think you should know about Inverse Adding-Doubling," Oregon Medical Laser Center, St. Vincent Hospital, 1–74 (2011).
32. G. M. Hale and M. R. Querry, "Optical Constants of Water in the 200-nm to 200-microm Wavelength Region," Appl. Opt. **12**(3), 555–563 (1973).
33. M. Daimon and A. Masumura, "Measurement of the refractive index of distilled water from the near-infrared region to the ultraviolet region," Appl. Opt. **46**(18), 3811–3820 (2007).
34. P. Giannios, S. Koutsoumpos, K. G. Toutouzas, M. Matiatou, G. C. Zografos, and K. Moutzouris, "Complex refractive index of normal and malignant human colorectal tissue in the visible and near-infrared," J. Biophotonics **10**(2), 303–310 (2017).
35. T. Naes, *et al*., *A user friendly guide to multivariate calibration and classification* (Chichester: NIR Publications, 2002).
36. R. Wehrens, *Chemometrics with R,* 1 ed., Use R! (Springer-Verlag Berlin Heidelberg, 2011).
37. H. Martens and E. Stark, "Extended multiplicative signal correction and spectral interference subtraction: new preprocessing methods for near infrared spectroscopy," J. Pharm. Biomed. Anal. **9**(8), 625–635 (1991).
38. R. C. Team, R: A Language and Environment for Statistical Computing, R Foundation for Statistical Computing, Vienna, Austria, 2015.
39. G. Schwarz, "Estimating the Dimension of a Model," Ann. Stat. **6**(2), 461–464 (1978).
40. L. Scrucca, M. Fop, T. B. Murphy, and A. E. Raftery, "mclust 5: Clustering, Classification and Density Estimation Using Gaussian Finite Mixture Models," R J. **8**(1), 289–317 (2016).
41. C. Fraley, A. Raftery, and L. Scrucca, "Normal mixture modeling for model-based clustering, classification, and density estimation," R Package Version 4(7) (2014).
42. M. Cope, "The application of near infrared spectroscopy to non invasive monitoring of cerebral oxygenation in the newborn infant," Dept. of Medical Physics and Bioengineering 342 (1991).

Biomedical Optics EXPRESS

43. S. G. Blumenthal, D. B. Taggart, R. D. Rasmussen, R. M. Ikeda, B. H. Ruebner, D. E. Bergstrom, and F. W. Hanson, "Conjugated and unconjugated bilirubins in humans and rhesus monkeys. Structural identity of bilirubins from biles and meconiums of newborn humans and rhesus monkeys," Biochem. J. **179**(3), 537–547 (1979).
44. M. A. Franceschini, S. Fantini, L. A. Paunescu, J. S. Maier, and E. Gratton, "Influence of a superficial layer in the quantitative spectroscopic study of strongly scattering media," Appl. Opt. **37**(31), 7447–7458 (1998).
45. J. J. D. Ostojic, H. Isler, S. Kleiser, T. Karen, M. Wolf, and F. Scholkmann, "Impact of skull thickness on cerebral NIRS oximetry in neonates: an in silico study," Adv. Exp. Med. Biol. in press.
46. S. L. Jacques, "Optical properties of biological tissues: a review," Phys. Med. Biol. **58**(11), R37–R61 (2013).
47. H. Liu, B. Chance, A. H. Hielscher, S. L. Jacques, and F. K. Tittel, "Influence of blood vessels on the measurement of hemoglobin oxygenation as determined by time-resolved reflectance spectroscopy," Med. Phys. **22**(8), 1209–1217 (1995).